An unliganded thyroid hormone receptor causes severe neurological dysfunction

Koshi Hashimoto*, Flavio H. Curty*, Patricia P. Borges*, Charlotte E. Lee†, E. Dale Abel†, Joel K. Elmquist†, Ronald N. Cohen*, and Fredric E. Wondisford*‡

*Section of Endocrinology and Metabolism, Department of Medicine, University of Chicago, Chicago, IL 60637; and †Division of Endocrinology and Metabolism, Department of Medicine, Beth Israel Deaconess Medical Center, and Harvard Medical School, Boston, MA 02215

Edited by Michael G. Rosenfeld, University of California at San Diego, La Jolla, CA, and approved December 26, 2000 (received for review September 21, 2000)

Congenital hypothyroidism and the thyroid hormone (T_3) resistance syndrome are associated with severe central nervous system (CNS) dysfunction. Because thyroid hormones are thought to act principally by binding to their nuclear receptors (TRs), it is unexplained why TR knock-out animals are reported to have normal CNS structure and function. To investigate this discrepancy further, a T_3 binding mutation was introduced into the mouse TR-β locus by homologous recombination. Because of this T_3 binding defect, the mutant TR constitutively interacts with corepressor proteins and mimics the hypothyroid state, regardless of the circulating thyroid hormone concentrations. Severe abnormalities in cerebellar development and function and abnormal hippocampal gene expression and learning were found. These findings demonstrate the specific and deleterious action of unliganded TR in the brain and suggest the importance of corepressors bound to TR in the pathogenesis of hypothyroidism.

Thyroid hormone (T_3) deficiency in early life affects central nervous system (CNS) development and function, resulting in decreased intelligence and movement disorders in humans. In rodent models of hypothyroidism, similar findings have been reported (1). Maternal hypothyroidism also has an impact on CNS development *in utero*, even when fetal thyroid function is normal (2). Finally, in patients with the syndrome of resistance to thyroid hormone (RTH), learning disorders and mental retardation have been reported (3). In this disorder, a mutant T_3 receptor (TR-β) expressed on one allele dominantly interferes with the function of the other TR isoforms (TR-β1, TR-β2, and TR-α1) and causes tissue hypothyroidism (3, 4).

To explore the mechanism of TR signaling *in vivo*, TR knock-out mouse models have been generated (5–9). Presumably in these models of tissue hypothyroidism, nuclear signaling should be abolished because of the lack of TRs. Paradoxically, however, these animals have a relatively mild phenotype compared with animals rendered hypothyroid by thyroid ablation and, apart from deafness caused by an inner ear defect (10), are reported to have normal CNS structure and function. This discrepancy suggests that the unliganded TR may play a central role in mediating the phenotypic changes of hypothyroidism in the CNS.

Materials and Methods

Generation of TR-β Mutant Mice. The mouse TR β genomic locus was isolated as a 70-kb clone from a 129/SvJ P1 genomic DNA library (Genome Systems, St. Louis). A mouse TR-β Exon 6 fragment was obtained with the use of the PCR and intronic primers flanking exon 6. This fragment was subcloned, and the Δ337T mutation was introduced by site-directed mutagenesis (CLONTECH). An *Eco*RI/*Bgl*II fragment, containing the exon 6 mutation, was assembled and subcloned into pGEM 7Z (Promega). A neomycin resistance gene cassette (NEO), driven by the phosphoglycerate kinase promoter, was inserted into intron 5 at an *Eco*RI site. Introduction of the NEO cassette resulted in a new *Bgl*II site in intron 5. The targeting construct in pGEM 7Z was linearized with *Sal*I before electroporation into embryonic stem cells derived from 129/SvJ mice (Genome Systems), and the cells were selected in media containing G418.

One hundred ninety-two G418-resistant colonies were screened with the use of Southern blot analysis and a 1-kb *Bgl*II/*Eco*RI radiolabeled probe from a region outside of the targeting vector in intron 4. Homologous recombination was detected in three clones, which were subsequently injected into blastocysts of the C57/BL6 strain. PCR with a Neo and an exon 7 oligonucleotide primer was performed on embryonic stem cell DNA from all three clones. PCR products were subcloned, and DNA sequencing confirmed the Δ337T mutation in the exon 6. Male chimeric mice were mated with female C57/BL6 mice as described (11), and germline transmission was obtained from all three clones. All mice were propagated in the C57/BL6 background strain, and direct comparisons were made with littermate controls.

All aspects of animal care were approved by the Institutional Animal Care and Use Committee of the Beth Israel Deaconess Medical Center (Boston, MA). Animals were maintained on a 12 h light/12 h dark schedule (light on at 06:00 h) and fed laboratory chow and water *ad libitum*.

RNA Analysis. Total RNA from tissues was isolated after homogenization in guanidinium thiocyanate. For Northern analysis, total RNA was fractionated in formaldehyde-containing agarose gels, transferred to nylon membrane (GeneScreen PLUS; NEN), and hybridized with a radiolabeled probe. For brain and cerebellum RNA samples, myelin basic protein (12), brain-derived neurotrophic factor (BDNF), and tyrosine protein kinase receptor B (TrkB) cDNA probes were used. The latter two cDNA probes were obtained by reverse transcription–PCR of total mouse brain. For the BDNF probe, a sense primer (nt 123–148) and an antisense primer (nt 654–629) were used (GenBank accession no. NM007540). For the TrkB probe, a sense primer (nt 121–146) and an antisense primer (−nt 648–623) were used (GenBank accession no. M33385). cDNA probes were confirmed by DNA sequencing.

RNase protection assays were performed (RPAIII kit; Ambion, Austin, TX) with the use of [α-^{32}P]UTP-labeled antisense riboprobes. The protected fragments were fractionated on a denaturing 6% polyacrylamide gel. For analysis of TR-β expression, a 500-bp genomic probe containing exon 6 and 5′ and 3′ intronic DNA was used. For analysis of c-erbA-α expression, a

This paper was submitted directly (Track II) to the PNAS office.

Abbreviations: T_3, thyroid hormone; TR, thyroid hormone receptor; RTH, resistance to thyroid hormone; CNS, central nervous system; BDNF, brain-derived neurotrophic factor; wt, wild type; TSH, thyroid-stimulating hormone; H&E, hematoxylin/eosin; Pcp-2, Purkinje cell protein-2; MBP, myelin basic protein; TrkB, tyrosine protein kinase receptor B.

‡To whom reprint requests should be addressed. E-mail: fwondisf@medicine.bsd.uchicago.edu.

The publication costs of this article were defrayed in part by page charge payment. This article must therefore be hereby marked "*advertisement*" in accordance with 18 U.S.C. §1734 solely to indicate this fact.

www.pnas.org/cgi/doi/10.1073/pnas.051454698

250-bp probe containing the A/B coding region of mouse c-erbA-α was used. In RNase protection assays, an antisense mouse cyclophilin riboprobe was included in the hybridization reaction as a control. Laser densitometry (Molecular Dynamics) was used to correct RNA levels with the use of this internal standard.

Gel Mobility Shift Assay. Gel mobility shift analysis of TR-β1 interactions was conducted with the nuclear hormone receptor interaction domains of N-CoR (human amino acids corresponding to murine 2063–2300) and SMRT (human amino acids 2098–2507). Wild-type (wt) and mutant TR-β1 proteins were derived from *in vitro* transcription/translation reactions in rabbit reticulocyte lysate (Promega). Interacting domains of the corepressors were synthesized as glutathione *S*-transferase fusion protein and column purified (13). Twenty nanograms of the indicated corepressor was used in the indicated lanes. Interactions were tested on a radiolabeled DR+4 element as previously described (14). In some lanes, T_3 was added at a concentration of 100 nM.

Serum Assays. Thyroid hormone levels (total and free T_3 and T_4) were measured in triplicate by radioimmunoassays (ImmuChem-coated tube kits; ICN). The thyroid-stimulating hormone (TSH) level was determined by a specific mouse TSH RIA (15), with the use of radiolabeled rat TSH antigen (reference preparation, AFP98991) and a mouse TSH-β antibody (hormone distribution program, National Institute of Diabetes and Digestive and Kidney Diseases, Bethesda, MD). Statistical comparisons used the unpaired *t* test.

Histology, Immunohistochemistry, and *in Situ* Hybridization. Brain samples from male mice at 3.5 weeks of the age ($n = 3$ per group) were excised and washed once with PBS and then fixed in 10% neutral-buffered formalin and embedded in paraffin, and 4–6-μm-thick sections were prepared and stained with hematoxylin/eosin (H&E). The cerebellar and molecular and Purkinje cell layer areas were quantitated on comparable sections by computer imaging with the use of SCION IMAGE Version 1.62 software (National Institutes of Health, Bethesda, MD).

For *in situ* hybridization and immunohistochemistry, mice were anesthetized with an i.p. injection of sodium pentobarbital, then perfused transcardially with 4% paraformaldehyde in PBS. Fourteen-micrometer-thick sections of brain in sagittal sections from each group of mice ($n = 3$ per group) were cut on a tabletop cryotome and mounted on Superfrost Plus glass slides (Fisher Scientific). Mouse anti-calbindin-D28k antibody (Sigma) was used for staining of Purkinje cells. To reduce background when this antibody was used, a M.O.M (Vector Laboratories) fluorescent kit was used. Purkinje cells were counted, based on the calbindin-D28k immunostaining, as the number of the cells per $\times$200 magnification field. Four different comparable fields for each genotype were used. For BDNF immunostaining, rabbit anti-BDNF (N-20) antibody (Santa Cruz Biotechnology) was used, and diaminobenzidine (Sigma) was used for visualization.

The protocol for *in situ* hybridization histochemistry has been described (16). An [α-[^{35}S]thio]UTP-labeled Purkinje cell protein-2 (*Pcp-2*) antisense riboprobe was synthesized from a mouse *Pcp-2* genomic DNA fragment (a kind gift from Dr. Noriyuki Koibuchi, Brigham & Women's Hospital, Boston, MA). The slides were exposed to Kodak Biomax MR film (Eastman Kodak) for 1–2 days. Slides were then dipped in NTB2 photographic emulsion (Eastman Kodak) and developed after 2 weeks of exposure, followed by counterstaining with thionin. Grain density in a Purkinje cells was quantitated by computer imaging with the use of SCION IMAGE Version 1.62 software (National Institutes of Health). Twenty cells from comparable fields for each genotype were measured.

Tests of CNS Function. The beam-balance task was used to assess the more complex components of vestibulomotor function and coordination as described for mice (17). Briefly, the mouse was placed on a narrow plastic beam (0.7 cm), and its ability to maintain equilibrium was scored as follows: 0, does not attempt to balance; 1, hangs on the beam and falls off; 2, hangs on the beam without falling; 3, hugs the beam without falling; 4, grasps the side of the beam and/or has unsteady movements; and 5, exhibits steady posture on the beam. Mice were pretrained twice, 24 h before the measurement.

The rotarod task for rats (18) was modified for use in mice (17). The rotarod device consists of a clear 36-mm-diameter motorized rod rotating at a speed of 18 rpm. Performance on the task was assessed by measuring the time until the mouse falls usboff or grips the device without attempting to walk on the rod. All mice were acclimated to the rotarod for 2 days before measurement.

The Morris water maze test involves a platform hidden in a round pan of opaque water. The apparatus and testing procedure for mice were previously described (5). Briefly, a pool was filled with water containing 10% (wt/vol) skimmed milk. A hidden platform was placed 1 cm below the water surface so that it was not visible to the mouse. Mice were pretrained twice on the apparatus, 1 day before the test.

Results

Generation and Characterization of TR Knock-in Mice. To prove the importance of the unliganded TR in mammalian development and function, we generated a knock-in model of tissue hypothyroidism. The RTH mutation (Δ337T, Fig. 1*a*) chosen for this study was found in a family where consanguineous parents each carried one mutant allele and their child was homozygous for this mutation (19). The parents showed a significant RTH phenotype, and the severely affected child succumbed to his disease at an early age. This mutation completely disrupts T_3 binding, resulting in constitutive repression of thyroid hormone-responsive genes (20). Based on the crystal structure of TR-α1, deletion of residue 337 located in β-strand 4 would be predicted to change the shape of the T_3 binding pocket and perhaps prevent ligand entry (21). This lack of T_3 binding would prevent dissociation of nuclear corepressors, N-CoR and SMRT, which normally mediate transcriptional repression and are released by T_3 (22, 23). Gel-shift analysis, in Fig. 1*b*, demonstrates the normal dissociation of corepressors from wt TR-β1 after the addition of ligand (T_3) and a lack of dissociation from the Δ337T mutant TR-β1. Similar results were obtained (data not shown) when this mutation was introduced into the rat TR-β1 isoform, which is virtually identical to mouse TR-β1. Therefore, regardless of the thyroidal state of the transgenic animal, this mutant TR-β should constitutively bind to corepressors.

As shown in Fig. 1*c*, this mutation was then introduced into the germline of mice by homologous recombination. In the targeting construct, a neomycin cassette was also included in the intron to allow for clonal selection. Three independent embryonic stem cell clones were obtained and injected into blastocysts. Germline transmission was confirmed from all clones by Southern blot analysis (Fig. 1*d*). To prove that this mutant allele was expressed at predicted levels, an RNase protection assay was performed with the use of a radiolabeled mouse TR-β exon 6 probe (Fig. 1*e*). wt (+/+) animals protected the full-length probe, but animals carrying either one (mut/+) or two (mut/mut) mutant alleles displayed a doublet band, consistent with digestion of the probe at the mutation site and the generation of two smaller bands of 133 bp and 126 bp. In mut/+ animals, there was an approximately equal RNA expression of the wt and mutant allele; as expected, the mutant allele was only found in mut/mut animals. Importantly, expression of the TR-β mutant did not affect expression of c-erbA-α isoforms including TR-α1 (Fig. 1*f*).

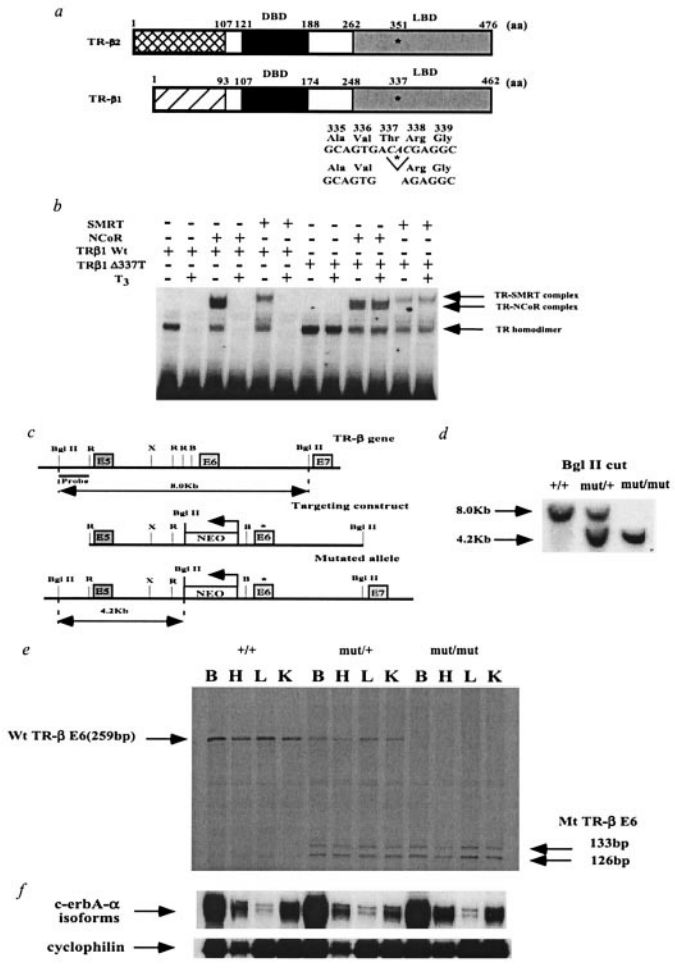

Fig. 1. Functional properties of the human mutation Δ337T and generation of TR-β knock-in mice by introduction of the human mutation Δ337T into the mouse TR-β locus. (*a*) Schematic representation of the TR-β isoforms and location of the Δ337T mutation in the mouse. Amino acid numbering is given for the human mutation in the mouse TR-β locus. Because this mutation is present in the ligand-binding domain (LBD), the mutation is present in both TR-β isoforms. DBD, DNA binding domain. (*b*) Gel mobility shift assay showing that the human Δ337T receptor mutant constitutively binds to corepressors (N-CoR, SMRT). T_3 was added at a concentration of 100 nM. (*c*) Introduction of Δ337T mutation into the mouse TR-β gene by homologous recombination. The asterisk marks the position of the Δ337T mutation in exon 6 (E6). The neomycin resistance gene (NEO), driven by the phosphoglycerate kinase promoter (bent arrow), was inserted into intron 5 in a direction opposite that of transcription as indicated. R, *Eco*RI; X, *Xba*I; B, *Bam*HI. (*d*) Homologous integration of the targeting vector was confirmed by Southern blot analysis of genomic DNA digested with *Bgl*II and probed with an α-^{32}P-labeled *Bgl*II-*Eco*RI probe located outside of the targeting vector. (*e*) Expression of the wt and mutant TR-β alleles in transgenic mice. RNase protection assays in various tissues were performed with a mouse exon 6 riboprobe. In mut/+ and mut/mut animals, the Δ337T mutation is located in the middle of exon 6. RNase treatment in these animals cleaved the probe into two smaller fragments (133 and 126 bps). Ten micrograms of total RNA from brain (B), heart (H), liver (L), and kidney (K) of 3-week-old male mice was analyzed. Because of the similar size of the control cyclophilin probe, it was hybridized to the same samples in a separate RNase protection assay. No significant differences were noted among these samples (data not shown). (*f*) RNase protection assay examining TR α1 with cyclophilin as a control. An N-terminal c-erbA-α probe was used in an RNase protection assay with cyclophilin as a control. Ten micrograms of total RNA from brain (B), heart (H), liver (L), and kidney (K) of 3-week-old male mice was analyzed. TR expression (β and α1) in the cerebellum was similar to that in whole brain (B) as shown in Fig. 1 *e* and *f* (data not shown).

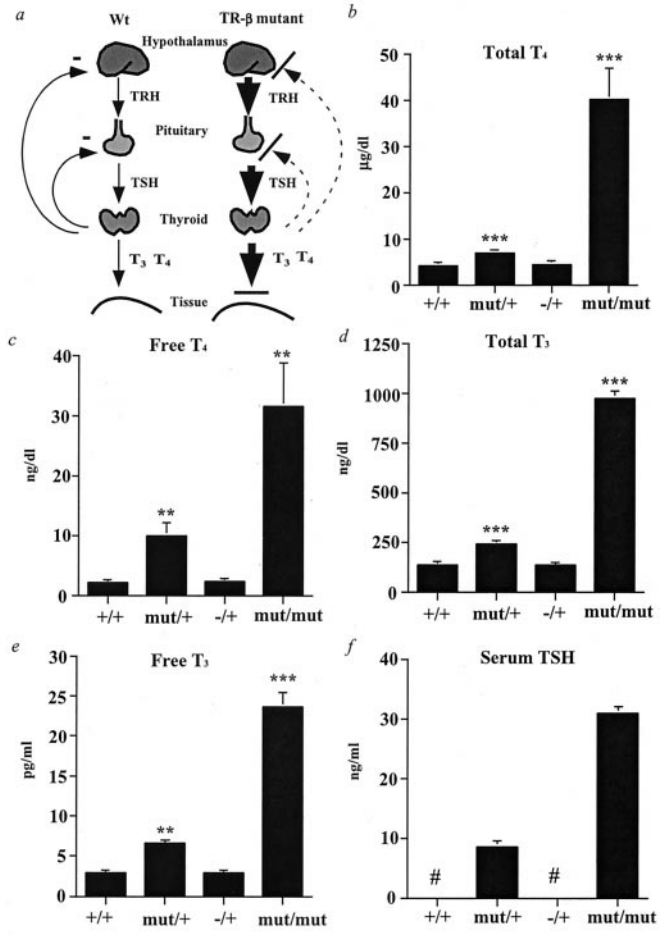

Fig. 2. Analysis of the hypothalamic–pituitary–thyroid axis in the TR-β mutant mice. (*a*) Schematic diagram of the axis and feedback loop in normal and TR-β mutant animals. The disruption in feedback at the hypothalamic TRH neuron is presumed but is not proven. (*b–f*) Serum total and free thyroid hormone and TSH levels (mean ± SEM) in serum from male mice at 4 weeks of age, as determined by RIA. +/+, $n = 11$; mut/+, $n = 14$; mut/mut, $n = 6$; TR-β −/+, $n = 6$. #, Below detection limit. **, $P < 0.01$ and ***, $P < 0.001$ vs. +/+ by *t* testing.

We found that mut/+ and mut/mut animals were similar in appearance, weight, and activity to wt animals. For example, their weight and growth were not different from wt animals up to 3 months of age (data not shown). We also found no decrease in litter size or viability of mut/+ and mut/mut animals versus wt animals.

Hypothalamus–Pituitary–Thyroid Axis in TR Knock-in Mice. We next determined the effect of this dominant negative mutation on the hypothalamic–pituitary–thyroid axis. As a control in this studies, we used TR-β knock-out mice, in which deletion of part of the DNA-binding domain of the TR-β locus results in the absence of expression of both TR-β isoforms (TR-β1 and TR-β2) (5). Mut/+ animals had significantly elevated serum TSH and total and free thyroid hormone levels (T_4 and T_3), indicating resistance to normal thyroid hormone negative feedback in the hypothalamus and pituitary (Fig. 2). These increased hormone levels are attributable to dominant inhibition of normal negative feedback mechanism, inasmuch as heterozygous TR-β knock-out animals (−/+) have normal serum TSH and thyroid hormone concentrations. A similar but more pronounced effect was noted in mut/mut animals, in which markedly elevated serum TSH and hormone levels were at least 3-fold higher than those

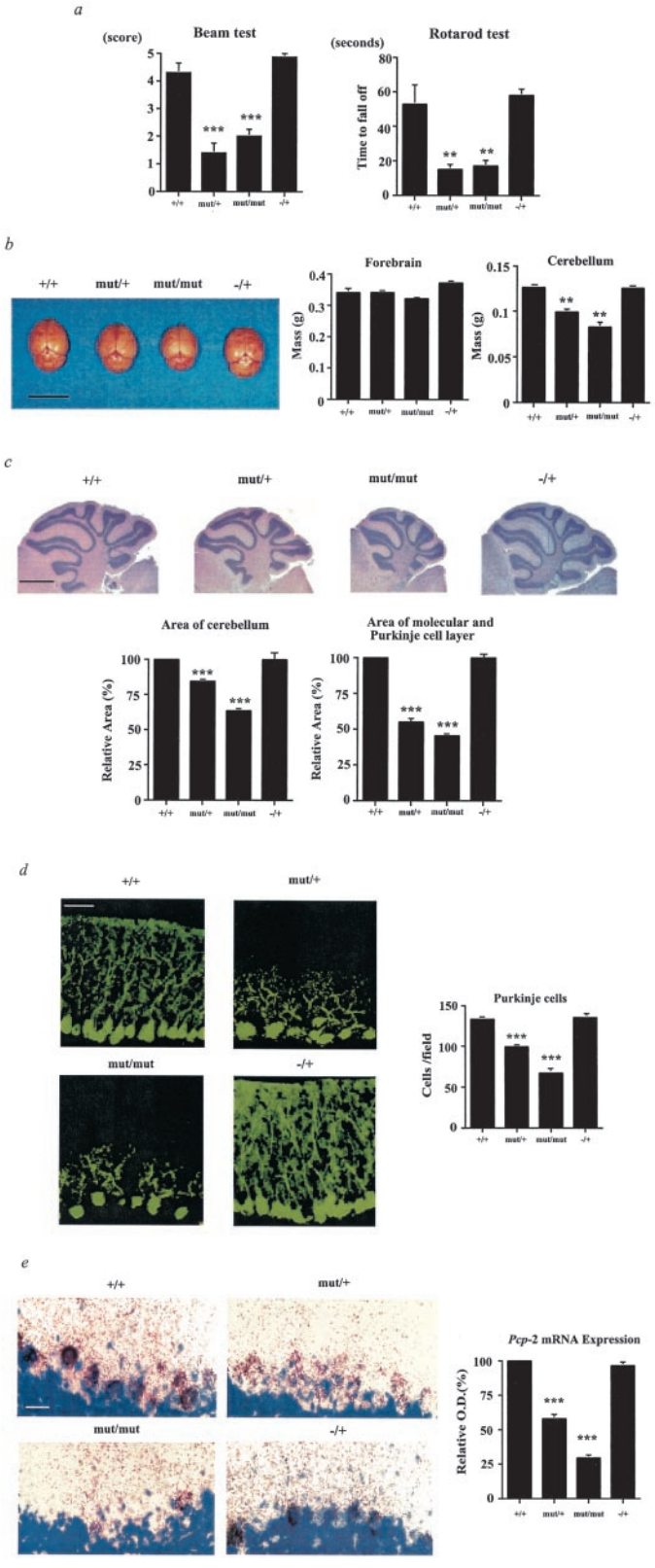

Fig. 3. Vestibulomotor function and cerebellar development in TR-β mutant animals. (*a*) Beam balance test and Rotarod test of male mice at 4 weeks of age (mean ± SEM). +/+, $n = 19$; mut/+, $n = 21$; mut/mut, $n = 15$; TR-β −/+, $n = 7$. Similar results have been obtained over several mouse generations (data not shown). (*b*) Brains of wt (+/+) and TR-β mutant animals (left side, 3.5 weeks old, male) and weight of their forebrain and cerebellum (right side, $n = 3$). (Scale bar = 1 cm.) (*c*) Hematoxylin and eosin staining and quantitation of area of mouse cerebellum and of molecular and Purkinje cell layers in mid sagittal section (3.5 weeks old, male). (Scale bar = 1 mm.) (*d*) Immunohistochemistry of mouse cerebellum (3.5 weeks old, male) with the use of an anti-calbindin-D28k antibody. (Scale bar = 50 μm.) Purkinje cell number was counted per ×200 magnification field. Four different comparable fields were used for each genotype. (*e*) *In situ* hybridization of mouse cerebellum with ^{35}S-labeled *Pcp-2* antisense riboprobe (3.5 weeks old, male). Black grains represent *Pcp-2* mRNA. The blue region is from counterstaining with thionin. (Scale bar = 50 μm.) The grain density in Purkinje cells is shown relative to the wt (+/+) animals in the bar graph. **, $P = < 0.01$ and ***, $P = < 0.001$ vs. +/+ by *t* testing.

reported in homozygous TR-β knock-out animals (5). The TR-α1 isoform must therefore play an important role in the control of this axis, as suggested from complete TR knock-out studies; however, the TR-α1 appears primarily to control the axis at the extremes of hormone secretion (8, 9). Whereas *in vivo* TR overexpression studies have suggested the importance of dominant negative inhibition in gene regulation (15, 24–26), these results obtained with allelic expression levels establish that dominant negative inhibition by TR is a physiologically important mechanism.

TR Knock-in Mice Exhibit Abnormalities in Cerebellar Function and Development. CNS structure and function were investigated in the TR-β mutant animals. Two tests of musculoskeletal function and balance were performed. TR-β mutant animals had marked impairment in balance and coordination (Fig. 3*a*, Beam and Rotarod tests) (17). These findings could be explained by abnormalities in cerebellar function, in which thyroid hormone is known to play an important developmental role (27). Interestingly, the cerebella of both mut/+ and mut/mut animals were smaller on gross sectioning and on H&E staining (Fig. 3 *b* and *c*). The mass of the cerebellum was reduced in mut/+ and mut/mut animals, but forebrain mass was normal, suggesting that the smaller cerebella of the knock-in animals were not because of an overall decrease in brain size. H&E staining suggested a decrease in the molecular and Purkinje cell layers in mut/+ and mut/mut animals. Based on this staining, we measured the area of the molecular and Purkinje cell layers. The sagittal area of cerebellum was decreased in mut/+ and mut/mut animals by 16% and 37% compared with +/+ and −/+ animals, respectively. On the other hand, the sagittal area of molecular and Purkinje cell layers was decreased to a greater extent in mut/+ and mut/mut animals by 46% and 55% compared with either the +/+ or +/− animals, respectively. This reduction in molecular and Purkinje cell layers was confirmed by immunohistochemistry for calbindin-D28k (Fig. 3*d*), suggesting that this reduction in molecular and Purkinje cell layers would explain the reduction in overall cerebellar size in the mutant animals. The calbindin-D28k staining also demonstrated a decrease in the number and branching of Purkinje cells in mut/+ and mut/mut animals.

In addition, *in situ* hybridization of mouse cerebella with a ^{35}S-labeled *Pcp-2* (28) antisense riboprobe was performed (Fig. 3*e*). *Pcp-2* mRNA expression levels in Purkinje cells were reduced in mut/+ and mut/mut animals by 42% and 71%, respectively. Moreover, an overall reduction in the number of Purkinje cells was also noted with this technique. In contrast, no abnormalities in *Pcp-2* expression or reduction in Purkinje cell number was found in the TR-β knock-out animals (29). Thus, the cerebella of mutant TR-β animals displayed findings observed in hypothyroid animals but not found or reported in TR knock-out animals (5–9).

TR Knock-in Mice Show a Learning Defect. To assess learning in the TR-β mutant mice, a Morris water maze test was used. In this test, a mouse is placed in the center of a circular pan of opaque

MEDICAL SCIENCES

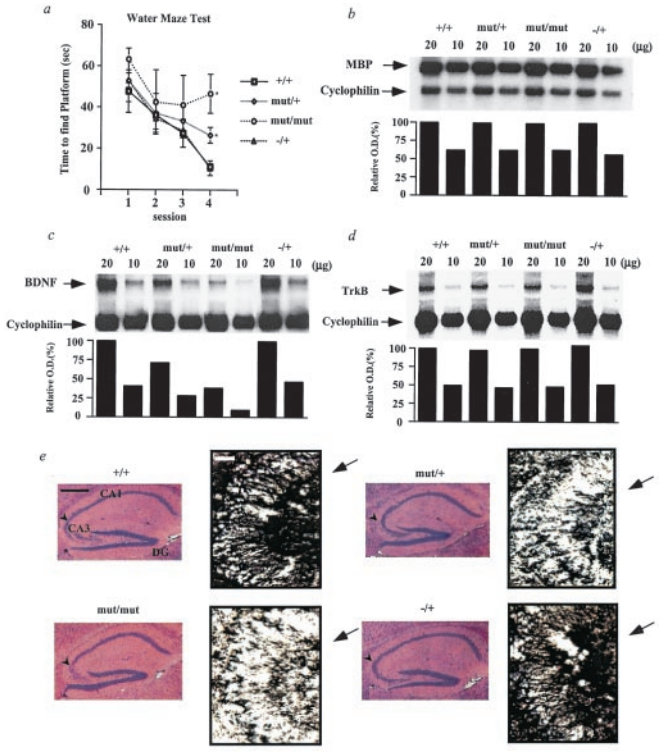

Fig. 4. Learning and gene expression in the cerebral cortex of TR-β mutant animals. (*a*) Spatial learning in the Morris water maze test. Male mice at 4 weeks of age [+/+ ($n = 20$), mut/+ ($n = 28$), mut/mut ($n = 10$), TR-β −/+ ($n = 6$)] were tested for their ability to learn to escape to a hidden platform. Data are expressed as mean time (in seconds) ± SEM. Mice were pretrained in two separate sessions 1 day before the test. Similar results have been obtained over several mouse generations (data not shown). (*b*) Northern blot analysis of myelin basic protein (MBP) mRNA levels in the cerebral cortex. (*c* and *d*) Northern blot analysis of brain-derived neurotrophic factor (BDNF) and its receptor (TrkB) mRNA levels in the anterior forebrain, respectively. (e) H&E staining of hippocampus (*Left*, scale bar = 0.5 mm) and immunostaining of hippocampal CA3 region with anti-BDNF antibody (*Right*, scale bar = 50 μm). (*Left*) The arrowhead indicates the CA3 region. (*Right*) The arrow indicates granule cell bodies stained by the anti-BDNF antibody. DG, dentate gyrus. *, $P = < 0.05$ vs. +/+ by *t* testing.

water. The time it takes for the mouse to find a hidden platform is recorded over daily sessions. As shown in Fig. 4*a*, wt animals (+/+) learn to find the platform sooner at each session, and TR-β −/+ (Fig. 4*a*) and TR-β −/− animals (5) perform like wt animals on this test. In contrast, both the mut/+ and mut/mut animals exhibited a learning defect in this test similar to that observed in congenitally hypothyroid animals (1). We cannot exclude the possibility that the cerebellar defect described above affected performance on the water maze test and confounded our assessment of learning in TR mutant animals. However, this test has been shown to be a valid tool for assessing learning in hypothyroid rodents based on the presence of otherwise normal swimming reflexes in congenitally hypothyroid rodents (reviewed in ref. 1). Thus, the dominant negative effect of the mutant receptor is also observed in CNS function. This observation, coupled with apparently normal CNS structure and function in the TR-α and TR-β knock-out mice (8, 9), suggests that the unliganded TR has a specific and deleterious effect on CNS structure and function.

To determine the mechanism of abnormal learning in the TR-β mutant mice, Northern blot analysis of steady-state mRNA levels for myelin basic protein (MBP), tyrosine protein kinase receptor B (TrkB), and brain-derived neurotrophic factor (BDNF) was performed on mRNA from the cerebral cortex or the anterior forebrain, as indicated (Fig. 4 *b–d*). MBP mRNA levels have been reported to be decreased in hypothyroid rodents at certain developmental time points (12). In TR-β mutant mice, we find no evidence that total MBP mRNA by Northern blot analysis (Fig. 4*b*) or MBP mRNA isoforms by RNase protection assay (data not shown) were decreased at 4 or 8 weeks of age. Moreover, the morphology of the cerebral cortex upon H&E staining and immunohistochemistry of the brain with an antibody against MBP revealed no differences among mutant and wt animals (data not shown). Thus, changes in cerebral cortex morphology or MBP expression cannot explain the learning defect observed in the TR-β knock-in mice.

Because the learning deficiency in these knock-in mice is identical to that described in mice with disruption of the BDNF signaling pathway in the hippocampus (30, 31), we next investigated the BDNF signaling pathway in the forebrain and hippocampus of mice. In the cerebellum, decreased BDNF expression during hypothyroidism has been linked to abnormal development (32), and BDNF expression in the cerebellum is stimulated by thyroid hormone (33). Consistent with the learning defect in TR-β mutant mice, BDNF mRNA levels were decreased in the forebrain by 30% in mut/+ animals and by 80% in mut/mut animals, as shown in Fig. 4*c*. In contrast, there was no change in the steady-state mRNA levels for TrkB, the receptor for BDNF (Fig. 4*d*). We also performed Northern blot analysis for both BDNF and TrkB expression in the cerebellum and obtained similar results. A 57% reduction in mut/+ and a 72% reduction in mut/mut animals in BDNF mRNA levels were found versus wt animals; TrkB mRNA levels were unchanged (data not shown).

As shown in Fig. 4*e*, H&E staining of the hippocampus/dentate gyrus revealed no gross morphological differences. BDNF protein distribution in hippocampus was examined in more detail with the use of immunohistochemical staining with anti-BDNF antibody. As shown in Fig. 4*e*, we found reduced immunoreactivity for BDNF in the hippocampus of both mut/+ and mut/mut animals versus wt and −/+ animals. The number of stained granule cells and fibers was especially reduced in the CA3 region of the hippocampus, as shown.

Discussion

In summary, TR-β knock-in mutant mice are phenotypically distinct from TR knock-out mutant mice. We provide evidence that the presence of a mutant unliganded TR-β mediates the phenotypic changes we describe in the hypothalamic–pituitary–thyroid axis and brain. The lack of similar changes in animals lacking one TR-β allele (−/+) in our studies and the lack of these reported defects in TR knock-out mice support the unique nature of these findings and indicate that dominant negative inhibition by a mutant TR is a physiologically relevant mechanism *in vivo*. Although the CNS of animals lacking all known TRs has not been evaluated to the same extent as TR-β knock-out and TR-β mutant animals, unpublished data suggest that they lack the CNS changes reported in the TR-β mutant animals [J. Samarut (Lyon, France), personal communication].

TR-β mutant mice display hypothyroid changes in the CNS despite elevated thyroid hormone levels. It is likely that elevated hormone levels in mutant TR-β mice mitigate changes in CNS structure and function by overcoming some of the dominant negative effects of the mutant TR-β on the remaining TR-α isoforms. Alternatively, elevated thyroid hormone levels acting through a nonnuclear pathway may contribute to the CNS phenotype in TR-β mutant animals, but this seems unlikely for two reasons. First, heterozygous TR-β mutant animals display elevations in thyroid hormone levels similar to those observed in homozygous TR-β knock-out animals, yet the latter animals have no reported CNS phenotype. Second, the CNS defects in

heterozygous versus homozygous TR-β mutant animals are similar, although their thyroid hormone levels are quite different. Thus, hyperthyroidism in TR-β mutant animals most likely lessens the severity of the CNS phenotype.

More generally, hypothyroidism and RTH are states of decreased thyroid hormone action in tissues due to lack of ligand or presence of an abnormal receptor, respectively. In the CNS, for example, patients with hypothyroidism and the RTH syndrome have significant defects in movement and learning. These abnormalities, however, have not been reported in knock-out animals lacking all known TRs (8, 9). TR bound to DNA is thought to repress gene transcription by recruiting a corepressor complex, which includes mSin3A and histone deacetylases (34, 35). The mutant TR-β in these animals functions similarly to the unliganded TR by constitutively binding to corepressors (20). Lower steady-state levels of *Pcp-2* and BDNF in the brain versus wt animals provides *in vivo* evidence of gene repression. These lower mRNA levels in TR-β mutant animals were observed even in the setting of elevated thyroid hormone levels in the mutant versus wt animals (Fig. 2). Conversely, data from *in vitro* studies predict that TR knock-out animals would lack the ability to repress gene transcription in the absence of thyroid hormone. This could explain the phenotypic differences between TR-β mutant versus TR knock-out animals. Thus, these data demonstrate the specific and deleterious action of an unliganded TR in mammalian development and function and suggest the importance of corepressors bound to TR in the pathogenesis of hypothyroidism.

We thank Drs. D. Forrest, M. J. Berry, N. Koibuchi, B. A. Hamilton, and C. N. Mariash for probes used in this study. The TR-β knockout mice were a kind gift of Dr. D. Forrest (Mount Sinai Medical School, New York). We also thank Dr. M. Mori (Gunma University School of Medicine, Maebashi, Japan) and Dr. S. Radovick (University of Chicago) for their advice and review of the manuscript. This work was supported by grants from the National Institutes of Health to F.E.W. (DK 49126 and DK 53036) and the Thyroid Research Advisory Council to E.D.A. F.H.C. and P.P.B. are recipients of Conselho Nacional de Pesquisas training funds from the government of Brazil.

1. Anthony, A., Adams, P. M. & Stein, S. A. (1993) *Horm. Behav.* **27,** 418–433.
2. Haddow, J. E., Palomaki, G. E., Allan, W. C., Williams, J. R., Knight, G. J., Gagnon, J., O'Heir, C. E., Mitchell, M. L., Hermos, R. J., Waisbren, S. E., *et al.* (1999) *N. Engl. J. Med.* **341,** 549–555.
3. Refetoff, S., Weiss, R. E. & Usala, S. J. (1993) *Endocr. Rev.* **14,** 348–399.
4. Lazar, M. A. (1993) *Endocr. Rev.* **14,** 184–193.
5. Forrest, D., Hanebuth, E., Smeyne, R. J., Everds, N., Stewart, C. L., Wehner, J. M. & Curran, T. (1996) *EMBO J.* **15,** 3006–3015.
6. Fraichard, A., Chassande, O., Plateroti, M., Roux, J. P., Trouillas, J., Dehay, C., Legrand, C., Gauthier, K., Kedinger, M., Malaval, L., *et al.* (1997) *EMBO J.* **16,** 4412–4420.
7. Wilkstrom, L., Johansson, C., Salto, C., Barlow, C., Campo Barros, A., Baas, F., Forrest, D., Thoren, P. & Vennstrom, B. (1998) *EMBO J.* **17,** 455–461.
8. Gauthier, K., Chassande, O., Plateroti, M., Roux, J. P., Legrand, C., Pain, B., Rousset, B., Weiss, R., Trouillas, J. & Samarut, J. (1999) *EMBO J.* **18,** 623–631.
9. Gothe, S., Wang, Z., Ng, L., Kindblom, J. M., Campo Barros, A., Ohlsson, C., Vennstrom, B. & Forrest, D. (1999) *Genes Dev.* **13,** 1329–1341.
10. Forrest, D., Erway, L. C., Ng, L., Altschuler, R. & Curran, T. (1996) *Nat. Genet.* **13,** 354–357.
11. Abel, E. D., Boers, M. E., Pazos-Moura, C., Moura, E., Kaulbach, H. C., Zakaria, M., Radovick, S., Liberman, M. C. & Wondisford, F. E. (1999) *J. Clin. Invest.* **104,** 291–300.
12. Farsetti, A., Mitsuhashi, T., Desvergne, B., Robbins, J. & Nikodem, V. M. (1991) *J. Biol. Chem.* **266,** 23226–23232.
13. Cohen, R. N., Putney, A., Wondisford, F. E. & Hollenberg, A. N. (2000) *Mol. Endocrinol.* **14,** 900–914.
14. Safer, J., Cohen, R. C., Hollenberg, A. N. & Wondisford, F. E. (1998) *J. Biol. Chem.* **273,** 30175–30182.
15. Abel, E. D., Kaulbach, H. C., Campos-Barros, A., Ahima, R. S., Boers, M. E., Hashimoto, K., Forrest, D. & Wondisford, F. E. (1999) *J. Clin. Invest.* **103,** 271–279.
16. Elmquist, J. K., Bjorbaek, C., Ahima, R. S., Flier, J. S. & Saper, C. B. (1998) *J. Comp. Neurol.* **395,** 535–547.
17. Scherbel, U., Raghupathi, R., Nakamura, M., Saatman, K. E., Trojanowski, J. O., Neugebauer, E., Marino, M. W. & McIntosh, T. K. (1999) *Proc. Natl. Acad. Sci. USA* **96,** 8721–8726.
18. Hamm, R. J., Pike, B. R., O'Dell, D. M., Lyeth, B. G. & Jenkins, L. W. (1994) *J. Neurotrauma* **11,** 187–196.
19. Usala, S. J., Menke, J. B., Watson, T. L., Wondisford, F. E., Weintraub, B. D., Berard, J., Bradley, W. E. C., Ono, S., Mueller, O. T. & Bercu, B. B. (1991) *Mol. Endocrinol.* **5,** 327–335.
20. Baniahmad, A., Tsai, S. Y., O'Malley, B. W. & Tsai, M. J. (1992) *Proc. Natl. Acad. Sci. USA* **89,** 10633–10637.
21. Wagner, R. L., Apriletti, J. W., McGrath, M. E., West, B. L., Baxter, J. D. & Fletterick, R. J. (1995) *Nature (London)* **378,** 690–697.
22. Horlein, A. J., Naar, A. M., Heinzel, T., Torchia, J., Gloss, B., Kurokawa, R., Ryan, A., Kamei, Y., Soderstrom, M., Glass, C. K., *et al.* (1995) *Nature (London)* **377,** 397–404.
23. Chen, J. D. & Evans, R. M. (1995) *Nature (London)* **377,** 454–457.
24. Hayashi, Y., Mangoura, D. & Refetoff, S. (1996) *Mol. Endocrinol.* **10,** 100–106.
25. Gloss, B., Sayen, M. R., Trost, S. U., Bluhm, W. F., Meyer, M., Swanson, E. A., Usala, S. J. & Dillmann, W. H. (1999) *Endocrinology* **140,** 897–902.
26. Pazos-Moura, C., Abel, E. D., Boers, M. E., Moura, E., Hampton, T. G., Wang, J., Morgan, J. P. & Wondisford, F. E. (2000) *Circ. Res.* **86,** 700–706.
27. Oppenheimer, J. H. & Schwartz, H. L. (1997) *Endocr. Rev.* **18,** 462–475.
28. Zou, L., Hagen, S. G., Strait, K. A. & Oppenheimer, J. H. (1994) *J. Biol. Chem.* **269,** 13346–13352.
29. Sandhofer, C., Schwartz, H. L., Mariash, C. N., Forrest, D. & Oppenheimer, J. H. (1998) *Mol. Cell. Endocrinol.* **137,** 109–115.
30. Linnersson, S., Bjorklund, A. & Ernfors, P. (1997) *Eur. J. Neurosci.* **9,** 2581–2587.
31. Minichiello, L., Korte, M., Wolfer, D., Kuhn, R., Unsicker, K., Cestari, V., Rossi-Arnaud, C., Lipp, H-P., Bonhoeffer, T. & Klein, R. (1999) *Neuron* **24,** 401–414.
32. Neveu, I. & Arenas, E. (1996) *J. Cell. Biol.* **133,** 631–646.
33. Koibuchi, N., Fukuda, H. & Chin, W. W. (1999) *Endocrinology* **140,** 3955–3961.
34. Heinzel, T., Lavinsky, R. M., Mullen, T. M., Soderstrom, M., Laherty, C. D., Torchia, J., Yang, W. M., Brard, G., Ngo, S. D., Davie, J. R., et al. (1997) *Nature (London)* **387,** 43–48.
35. Nagy, L., Kao, H. Y., Chakravarti, D., Lin, R. J., Hassig, C. A., Ayer, D. E., Schreiber, S. L. & Evans, R. M. (1997) *Cell* **89,** 373–380.